Ground-State Geometry Preferences in (Tris(pyrazolyl)borato)- and Cyclopentadienylniobium Alkyne Complexes

Michel Etienne,*,† Bruno Donnadieu,† René Mathieu,† Juan Fernández Baeza,‡ Felix Jalón,‡ Antonio Otero,‡ and Maria Esther Rodrigo-Blanco‡

Laboratoire de Chimie de Coordination du CNRS, UPR 8241, 205 Route de Narbonne, 31077 Toulouse Cedex, France, and Departamento de Química Inorgánica, Orgánica y Bioquímica, Facultad de Ciencias Químicas, Universidad de Castilla-La Mancha, Campus Universitario, 13071 Ciudad Real, Spain

Received May 24, 1996[⊗]

Reaction of $NbCl_3(DME)(RC{\equiv}CR')$ with KTp (DME = 1,2-dimethoxyethane, Tp = hydrotris(pyrazolyl)borate) yields $TpNbCl_2(RC{\equiv}CR')$ (R = Ph, R′ = Me (**2a**); R = R′ = Me (**2b**), Et (**2c**), $SiMe_3$ (**2d**), Ph (**2e**)), which has the alkyne in the molecular mirror plane in the solid state (X-ray crystal structure for **2a**) and in solution. The barriers to alkyne rotation are low, the highest being measured for complex **2d** (52 kJ mol^{-1} at 273 K), which contains the bulky $SiMe_3$ group on the alkyne. In TpCpNb(Cl)(PhC≡CMe) (**3a**), formed by reaction of **2a** with NaCp·DME, the alkyne is parallel to the Cp plane, as observed in solution and in the crystal structure. Extended Huckel molecular orbital calculations indicate that in complexes **2** the geometry is mainly governed by steric interactions, whereas in the case of **3a** orbital interactions dictate the observed geometry.

Introduction

Competition between ligands for available metal orbitals is evidenced by different possible ligand orientations, but steric effects also have to be taken into account. We have fully characterized the niobium complexes $Tp^*NbCl_2(RC{\equiv}CR')$ (**1**; Tp* = hydrotris(3,5-dimethylpyrazolyl)borate) in which the four-electron (4e) donor alkyne[1] lies in the molecular mirror plane.[2] In the isoelectronic cyclopentadienyl (Cp) series $CpMX_2(RC{\equiv}CR)$ (M = Nb, Ta) the geometry is known to be orthogonal so that the alkyne is parallel to the Cp plane.[3,4] We initially proposed[2a] that the main reason for this difference rested on steric grounds, and we recently provided a qualitative molecular orbital model that confirmed this proposal.[2b] We then thought that a direct experimental assessment of steric versus orbital control could be achieved by replacing the bulky Tp* ligand by the unsubstituted Tp ligand (Tp = hydrotris(pyrazolyl)borate). Furthermore, the presence of both a Tp and a Cp ligand in a single complex would be desirable so that the influence of the two ligands could also be probed intramolecularly. This article describes solid-state and solution studies on $TpNbCl_2(RC{\equiv}CR')$ as well as the full characterization of the mixed TpCp complex TpCpNbCl(PhC≡CMe). In the former case, the alkyne orientation is identical with that in the Tp* complex, whereas in the latter, addition of the Cp ligand to the niobium coordination sphere results in the reorientation of the alkyne parallel to the Cp plane. These preferences are analyzed with the help of extended Hückel molecular orbital (EHMO) calculations.

Results and Discussion

Hydrotris(pyrazolyl)borato Complexes. The red-purple Tp complexes $TpNbCl_2(RC{\equiv}CR')$ (R = Ph, R′ = Me (**2a**); R = R′ = Me (**2b**), Et (**2c**), $SiMe_3$ (**2d**), Ph (**2e**)) have been synthesized by the reaction of $NbCl_3(DME)(RC{\equiv}CR')$[5] (DME = 1,2-dimethoxyethane) with KTp are previously described from complexes **1** (eq 1).[2] An X-ray

$$NbCl_3(DME)(RC{\equiv}CR') + KTp \xrightarrow{thf} \mathbf{2} \quad (1)$$

crystal structure of **2a** leads to the view shown in Figure 1. A summary of crystal data is provided in Table 1, and relevant bond distances and angles can be found in Table 2. The short niobium-coordinated alkyne carbon bonds (Nb(1)−C(2) = 2.065(6) Å; Nb(1)−C(3) =

† Laboratoire de Chimie de Coordination du CNRS. E-mail for M.E.: etienne@lcc-toulouse.fr.

‡ Universidad de Castilla-La Mancha.

⊗ Abstract published in *Advance ACS Abstracts,* August 15, 1996.

(1) Templeton, J. L. *Adv. Organomet. Chem.* **1989**, *29*, 1.

(2) (a) Etienne, M.; White, P. S.; Templeton, J. L. *Organometallics* **1991**, *10*, 3801. (b) Etienne, M.; Biasotto, F.; Mathieu, R.; Templeton, J. L. *Organometallics* **1996**, *15*, 1106.

(3) (a) Curtis, M. D.; Real, J. *Organometallics* **1985**, *4*, 940. (b) Curtis, M. D.; Real, J.; Kwon, D. *Organometallics* **1989**, *8*, 1644. (c) Smith, G.; Schrock, R. R.; Churchill, M. R.; Youngs, W. *Inorg. Chem.* **1981**, *20*, 387. (d) Belmonte, P. A.; Cloke, F. G. N.; Theopold, K. H.; Schrock, R. R. *Inorg. Chem.* **1984**, *23*, 2365.

(4) The only exception is the case of the benzyne ligand; see: (a) McLain, S. J.; Schrock, R. R.; Sharp, P. R.; Churchill, M. R.; Youngs, W. J. *J. Am. Chem. Soc.* **1979**, *101*, 263. (b) Churchill, M. R.; Youngs, W. J. *Inorg. Chem.* **1979**, *18*, 1697.

(5) Hartung, J. B.; Pedersen, S. F. *Organometallics* **1990**, *9*, 1414.

S0276-7333(96)00404-9 CCC: $12.00

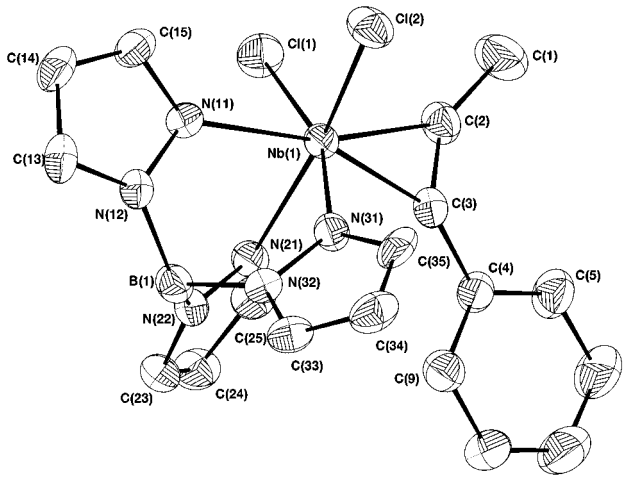

Figure 1. Perspective view of complex **2a**.

Table 1. Crystal Data, Data Collection, and Refinement Parameters for TpNbCl$_2$(PhC≡CMe)·thf (2a·thf) and TpCpNbCl(PhC≡CMe) (3a)

	2a·THF	**3a**
	Crystal Data	
chem formula	$C_{22}H_{18}Cl_2N_6BNbO$	$C_{23}H_{23}ClN_6BNb$
fw	541	535
cryst syst	monoclinic	monoclinic
space group	$P2_1/n$	$P2_1/n$
a (Å)	11.630(3)	9.140(3)
b (Å)	8.829(2)	15.176(9)
c (Å)	24.929(5)	16.644(9)
β (deg)	100.29(1)	90.65(4)
V (Å^3)	2525(1)	2307(2)
Z	4	4
ρ(calcd) (Mg m^{-3})	1.423	1.54
cryst size (mm)	0.45 × 0.30 × 0.25	0.5 × 0.27 × 0.2
μ (cm^{-1})	6.889	6.40
	Data Collection	
radiation (graphite monochr)	Mo Kα (λ = 0.710 73 Å)	
data collecn method	$\omega/2\theta$	
no. of measd rflns	5512	7162
no. of merged rflns (R_m)	4183 (0.0486)	6711 (0.0479)
no. of obsd rflns	4722 ($I > 3\sigma(I)$)	4645 ($I > 3\sigma(I)$)
2θ range (deg)	$3 < 2\theta < 50$	$3 < 2\theta < 60$
range of hkl	$+13 \geq h \geq -13$, $10 \geq k \geq 0$, $29 \geq l \geq 0$	$+12 \geq h \geq -12$, $21 \geq k \geq 0$, $23 \geq l \geq 0$
scan range θ (deg)	0.8 + 0.345 tan θ	0.9 + 0.345 tan θ
	Refinement	
refinement on	F	
R^a	0.0409	0.0290
$R_w{}^b$	0.0464	0.0338
ls params	262	295
abs cor	Difabs	
min/max cor	0.75−1.00	0.67−1.00
weighting scheme	1	1
goodness of fit, S^c	2.5	1.9
residual electron density (e Å^{-3})	±0.5	±0.4

^{a} $R = \Sigma(||F_o| - ||F_c||)/\Sigma|F_o|$. ^{b} $R_w = [\Sigma w(||F_o| - |F_c||)^2/\Sigma(|F_o|)^2]^{1/2}$. ^{c} Goodness of fit $S = [\Sigma(|F_o - F_c|)^2/(N_{observns} - N_{parms})]^{1/2}$.

2.071(6) Å) and the elongated coordinated C−C bond (C(2)−C(3) = 1.301(8) Å) point to a 4e-donor description for the alkyne.[1] The alkyne lies in the molecular mirror plane which bisects the Cl−Nb−Cl angle and the N−Nb−N angle of the two *cis* pyrazole rings. This geometry is identical with that found previously for the Tp* analog Tp*NbCl$_2$(PhC≡CMe) (**1a**),[2] and the metric parameters are only marginally different in the two structures. However, the ^{1}H NMR room-temperature

Table 2. Selected Bond Lengths (Å) and Angles (deg) for TpNbCl$_2$(PhC≡CMe) (2a) (Esd's in Parentheses)

	Bond Lengths		
Nb(1)−Cl(1)	2.389(2)	Nb(1)−N(11)	2.306(5)
Nb(1)−Cl(2)	2.389(2)	Nb(1)−N(21)	2.222(5)
Nb(1)−C(2)	2.065(6)	Nb(1)−N(31)	2.241(5)
Nb(1)−C(3)	2.071(6)	C(2)−C(3)	1.301(8)
	Bond Angles		
C(1)−C(2)−C(3)	143.1(7)	C(2)−C(3)−C(4)	140.5(6)
Cl(1)−Nb(1)−Cl(2)	101.33(7)	N(21)−Nb(1)−N(31)	80.1(2)

spectrum of **2a** only shows one set of signals in a 1:2 ratio for each type of Tp hydrogens and one alkyne methyl resonance. This indicates (i) a plane of symmetry in **2a** (as in the solid state) and (ii) either a single isomer or rapid rotation about the niobium−alkyne bond. Although the slow exchange limit has not been reached, the latter proposal is correct since a coalescence of the alkyne methyl signal is observed at *ca*. 178 K in the ^{1}H NMR spectrum. In the 2-butyne complex TpNbCl$_2$(MeC≡CMe) (**2b**) single alkyne methyl and alkyne carbon resonances are found in both the ^{1}H and ^{13}C NMR spectra, whatever the temperature. In the ^{1}H NMR spectrum of the bis(trimethylsilyl)ethyne complex TpNbCl$_2$(Me$_3$SiC≡CSiMe$_3$) (**2d**), coalescence of the trimethylsilyl signals occurs at 273 K, leading to a barrier to alkyne rotation of 52 kJ mol^{-1}. For the Tp* analogs, much higher barriers are found. For **1a**, two rotamers are observed up to 373 K and the lower measurable barrier (68 kJ mol^{-1} at 358 K) is observed for the 2-butyne complex **1b**.[2]

Thus, it may be concluded that tris(pyrazolyl)borate coordination defines the geometry of the ground state, whereas the energy of the barrier to alkyne rotation is largely determined by the steric demand of either the pyrazolyl groups or the alkyne substituents.

Another difference between Tp and Tp* complexes resides in their electrochemical behavior, as briefly studied by cyclic voltammetry (scan rate 0.1 V s^{-1}). The phenylpropyne complex **1a** undergoes a quasi-reversible one-electron reduction at −1.19 V (versus SCE) with a peak-to-peak separation of 0.15 V and a peak intensity ratio of 0.9. For the Tp congener **2a** these parameters are respectively −0.93 V, 0.25 V, and 0.5. This is consistent with Tp* being more electron rich than Tp but also with the idea that Tp* imparts more kinetic stability than Tp, undoubtedly mainly for steric reasons. Similar observations and conclusions have been made in inorganic vanadium chemistry.[6]

A Cyclopentadienyl Hydrotris(pyrazolyl)borato Complex. Reacting complex **2a** with NaCp·DME in thf affords the yellow mixed TpCp complex TpCpNbCl(PhC≡CMe) (**3a**) in 75% yield (eq 2). A similar reaction does not occur in the Tp* case, presumably for steric reasons. Virtually invariant NMR data between 193 and 353 K show that the Cp is η^5-bound, that the Tp is η^3-bound, and that a 2e-donor description for the niobium−alkyne interaction is appropriate (δ 163.5 and 152.9 for the coordinated alkyne carbons in the major isomer).[1,7] Two discrete isomers are observed in a 1:5 ratio with no evidence of interconversion in this temperature range. Thus, the barrier to isomer interconversion, *i.e.*, to alkyne rotation, is at least 85 kJ mol^{-1}.

(6) Mohan, M.; Holmes, S. M.; Butcher, R. J.; Jasinski, J. P.; Carrano, C. J. *Inorg. Chem.* **1992**, *31*, 2029.

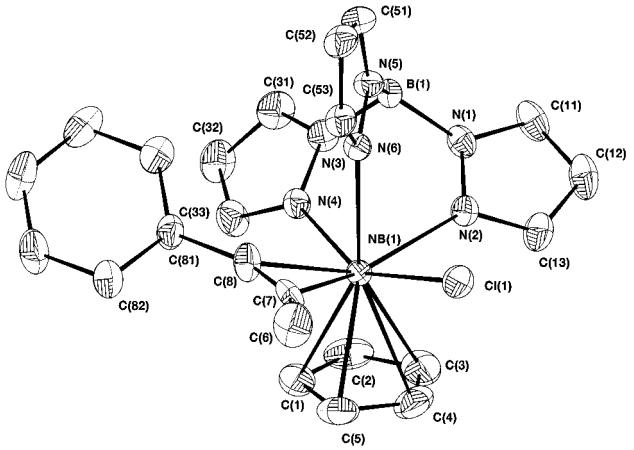

Figure 2. Perspective view of complex **3a**.

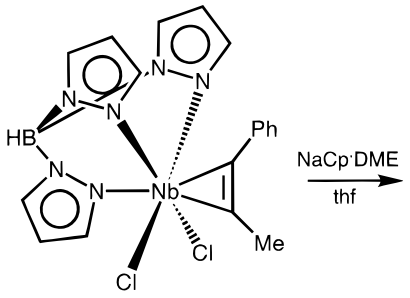

2a

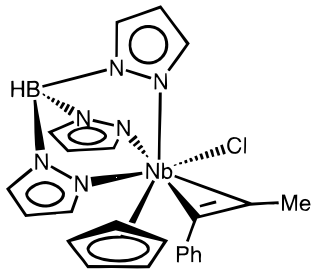

3a (2)

Complex **3a** has formally 18 valence electrons with a Nb^{III} d^2-center.

The crystal structure of **3a** is shown in Figure 2. A summary of crystal data is provided in Table 1, and relevant bond distances and angles can be found in Table 3. The overall description of the structure agrees with the solution data, although a single isomer is observed in the crystal. The Tp ligand is η^3-bound, and the Cp ligands is η^5-bound with virtually no slippage. The coordination sphere has long bonds to all ligands, a consequence of both increased steric crowding and an increased electron count at niobium. Nb(1)—N(4) is only slightly (*ca.* 0.02 Å) longer than the other two niobium—pyrazole nitrogen bonds. Angles around the niobium between the Cp centroid C(100) and the two cisoid nitrogens are 99.5(2) and 102.2(2)°; that between the Cp centroid C(100) and the transoid nitrogen N(6) is 172.9(2)°. Similar angular values have been observed in $CpTpZrCl_2$ and $CpTpZr(OC_6H_4Ph\text{-}2)_2$,[8,9] two rare examples of mixed TpCp complexes. The coordinated C—C bond of the alkyne is short (C(7)—C(8) = 1.254(4) Å), and the Nb—C bonds to the coordinated alkyne are long (Nb(1)—C(7) = 2.146(3) Å; Nb(1)—C(8) = 2.165(3) Å), in accord with a two-electron (2e) donor behavior for this ligand.[1,7] These parameters compare well with those for $(\eta^5\text{-}C_5H_4SiMe_3)_2Nb(Cl)(PhC{\equiv}CPh)$ (Nb—C = 2.171(8), 2.185(9) Å; C—C = 1.27(1) Å)[7a] and differ markedly from those for complex **2a**.

Table 3. Selected Bond Lengths (Å) and Angles (deg) for TpCpNbCl(PhC≡CMe) (3a) (Esd's in Parentheses)

Bond Lengths[a]			
Nb(1)—Cl(1)	2.5357(8)	Nb(1)—N(4)	2.303(2)
Nb(1)—C(7)	2.146(3)	Nb(1)—N(6)	2.324(2)
Nb(1)—C(8)	2.165(3)	C(7)—C(8)	1.254(4)
Nb(1)—N(2)	2.321(2)	Nb(1)—C(100)	2.157(3)

Bond Angles[a]			
C(6)—C(7)—C(8)	143.2(3)	C(7)—C(8)—C(81)	141.5(3)
Cl(1)—Nb(1)—C(7)	77.81(9)	Cl(1)—Nb(1)—C(8)	108.76(9)
C(100)—Nb(1)—N(4)	99.5(1)	C(100)—Nb—N(2)	102.2(1)
C(100)—Nb(1)—N(6)	172.8(1)	C(100)—Nb(1)—Cl(1)	104.3(1)

[a] C(100) is the centroid of the Cp ring.

Perhaps the most interesting part of the structure is the alkyne orientation. Indeed, the phenylpropyne (except the phenyl ring, which still sits upright in the wedge formed by two pyrazole rings) lies almost parallel to the Cp plane (dihedral angle 17.1°) so that it is no longer bisecting two *cis* pyrazole rings as in **2a**. In this conformation, the coordinated C—C bond of the alkyne eclipses the Nb(1)—N(4) bond. Atoms Cl(1), Nb(1), and the coordinated alkyne carbons C(7) and C(8) are close to coplanar,[10] so that this geometry is somewhat reminiscent of that observed in the bent-metallocene series Cp_2MXL (M = Nb, Ta), where ligands X and L (olefins, alkynes, etc.) lie in the wedge formed by the bent Cp_2M moiety, with two possible *exo* and *endo* isomers.[7,11] The angle between the planes defined by the Cp ring and the three coordinated nitrogen atoms is 127.6°. It is fully comparable to the Cp—Nb—Cp angle of 128.4° measured for $(\eta^5\text{-}C_5H_4SiMe_3)_2Nb(Cl)(PhC{\equiv}CPh)$.[7a]

Thus, we are in the peculiar situation whereby in the case of 16-electron Nb^{III} d^2 species with 4e-donor alkyne ligands, either the Tp or Cp ligand independently dictates a different geometry for the ground state whereas, in 18-electron Nb^{III} d^2 complexes with a 2e-donor alkyne, the direct intramolecular competition between Tp and Cp ligands leads to a Cp-driven orientation of the alkyne. In order to analyze the main reasons for these geometrical preferences, EHMO calculations have been performed.

EHMO Calculations. The EHMO calculations have been carried out for the two model complexes $TpNbCl_2(HC{\equiv}CH)$ and TpCpNbCl(HC≡CH). The bond lengths and angles were taken from the X-ray crystal structures of **2a** and **3a**, respectively.

(7) (a) Antinolo, A.; Gomez-Sal, P.; Martinez de Lladuya, J.; Otero, A.; Royo, P.; Martinez Carrera, S.; Garcia Blanco, S. *J. Chem. Soc., Dalton Trans.* **1987**, 975. (b) Serrano, R.; Royo, P. *J. Organomet. Chem.* **1983**, *247*, 33. (c) Fredericks, S.; Thomas, J. L. *J. Am. Chem. Soc.* **1978**, *100*, 350. (d) For a comparison of different alkyne behaviors in group 5 complexes, see: McGeary, M. J.; Gamble, A. S.; Templeton, J. L. *Organometallics* **1988**, *7*, 271. Lorente, P.; Etienne, M.; Donnadieu, B. *An. Quim. Int. Ed.* **1996**, *92*, 88.

(8) Reger, D. L.; Mahtab, R.; Baxter, J. C.; Lebioda, L. *Inorg. Chem.* **1986**, *25*, 2046.

(9) Kresinski, R. A.; Hamor, T. A.; Jones, C. J.; McCleverty, J. A. *J. Chem. Soc., Dalton Trans.* **1991**, 603.

(10) The deviations from the least-squares plane are as follows (Å): C(7), −0.206; C(8), 0.198; Nb(1), 0.103; Cl(1), −0.095. The coordinated carbons in $(\eta^5\text{-}C_5H_4SiMe_3)_2Nb(Cl)(PhC{\equiv}CPh)$ are 0.093(7) and −0.106(8) Å away from the molecular plane.[7a]

(11) Lauher, J. W.; Hoffmann, R. *J. Am. Chem. Soc.* **1976**, *98*, 1729. See also: Green, J. C.; Green, M. L. H.; Prout, C. K. *J. Chem. Soc., Chem. Commun.* **1972**, 421.

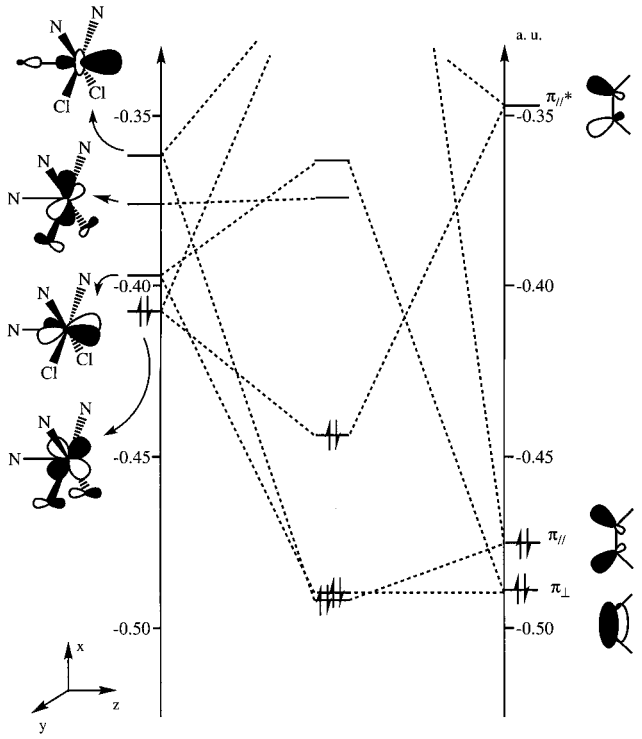

Figure 3. Molecular orbital diagram for the model compound $TpNbCl_2(HC{\equiv}CH)$ (1 au = 27.2 eV).

Let us start with $TpNbCl_2(HC{\equiv}CH)$. Recently,[2b] we qualitatively discussed the bonding in the Tp* analogs of complexes **2**, and the results of the calculations corroborate this view. In a first approximation, $TpNbCl_2$ is an ML_5 fragment of virtually cylindrical symmetry with no π-acceptor ligand. Subsequent breaking of the symmetry only leads to small perturbations. This cannot induce large splittings in the d_π set, and consequently no clear preference for π-bonding in one plane or the other occurs. Figure 3 shows the results of the calculations for the observed bisecting geometry. In order of increasing energy, the frontier molecular orbitals of $TpNbCl_2$ are essentially the d_{xz}, d_{yz}, $d_{x^2-y^2}$ and d_{z^2}, the last being a σ-type orbital (d_σ). The remaining d_{xy} orbital gives strong σ bonds with nitrogen and chlorine orbitals and is consequently not shown. Significant π-mixing with chlorine p orbitals are to be noted for d_{xz}, d_{yz}, and $d_{x^2-y^2}$. The d_σ orbital contains some niobium p_z character and is σ-antibonding with the pyrazole nitrogen along the *z* axis. Thus, this orbital points toward the alkyne and has the correct symmetry to interact with the alkyne $\pi_{||}$. This orbital is filled in the complex. The lengthening of the Nb−N bond along the *z* axis, as observed in the crystal structures of **1a** and **2a**, is a direct consequence of populating this orbital. The other occupied alkyne orbital $\pi_\perp$ gives a π-interaction with d_{yz}, the bonding linear combination of which is low in energy (this orbital does not appear to be stabilized toward $\pi_\perp$ in the alkyne because there are some symmetry-related pyrazole-based orbitals which elevate its energy). The second π-interaction occurs between the antibonding alkyne $\pi_{||}$* and the d_{xz} orbital. In our d^2 system, the bonding combination constitutes the HOMO. The LUMO of the complex is $d_{x^2-y^2}$, which remains essentially unchanged in a nonbonding situation. The computed HOMO−LUMO gap is 1.9 eV, leading to a configurationally stable 16-electron diamagnetic complex.

When the alkyne is rotated by 90° (horizontal geometry), the total energy only increases by 0.2 eV, a HOMO−LUMO gap of 1.7 eV being computed. Hence, we see that there is virtually no orbital preference for one geometry over the other. This stems from the small splitting between the two orthogonal π-type orbitals d_{xz} and d_{yz}, which give similar interactions with the alkyne $\pi_\perp$ and $\pi_{||}$* as the alkyne rotates.

Preference for the bisecting geometry may result from two complementary factors. In the horizontal geometry, there are obvious unfavorable steric interactions between the alkyne carbons and the pyrazole substituent at the 3-position. These interactions are alleviated in the bisecting geometry. Furthermore, electronic interactions between the π-systems of the two *cis*-pyrazole rings and one of the alkyne substituents are effective. This is especially the case when this substituent is a phenyl group, and this conformation is observed in the solid-state structures of **1a** and **2a**. Both factors influence the height of the barrier to alkyne rotation, as indicated above.

Curtis and co-workers[3b] previously performed EHMO calculations on the related Cp complex $CpNbCl_2(HC{\equiv}CH)$, which adopts the horizontal geometry. Basically the same orbital scheme is found for both compounds. The nature of the LUMO is different (certainly due to the fact that Tp polarizes the d orbitals toward the octahedral geometry), but the HOMO−LUMO gaps and the splittings between the two highest occupied orbitals are strikingly similar. For $CpNbCl_2(HC{\equiv}CH)$, a small barrier to alkyne rotation was computed (6 kcal mol^{-1}), indicating that the vertical geometry is easily accessible. Recall here that the benzyne derivative Cp^*TaMe_2(benzyne) has the alkyne in the molecular mirror plane, *i.e.*, the vertical geometry is preferred.[4] The vertical orientation of the alkene in the d^6 iridium complex $TpIrH_2$(cyclooctene) has been shown to result from orbital control,[12] although through a complex mechanism. For the d^4 tungsten complex $[Tp^*W(CO)_2(PhC{\equiv}CMe)]^+$, the dicarbonyl system forces the alkyne to lie in the symmetry plane of the complex.[13]

A very different situation is encountered for TpCpNbCl(HC≡CH). First of all, there is no symmetry in this complex and, thus, various mixing of orbitals complicates the analysis. However, upon removal of the alkyne, we are left with the d^2 fragment TpCpNbCl, which is of low symmetry as well. The frontier orbitals and energy levels are shown in Figure 4. The HOMO of the fragment is ideally suited to interact with the alkyne $\pi_{||}$* to give a π-type orbital, transferring electron density to the alkyne. Interestingly, this π-orbital remains the HOMO when the alkyne complex is formed. The LUMO of the unsaturated fragment is a σ-type orbital which has the correct symmetry to overlap with the alkyne $\pi_{||}$. These interactions represent the basis of a formal 2e-donor behavior of the alkyne. At somewhat higher energies we found two other orbitals of the fragment with strong d character. The lower energy orbital lies in a plane orthogonal to the pyrazole ring *trans* to the Cp and has no orbital mate on the alkyne.

(12) Bovens, M.; Gerfin, T.; Gramlich, V.; Petter, W.; Venanzi, L. M.; Haward, M. T.; Jackson, S. A.; Eisenstein, O. *New J. Chem.* **1992**, *16*, 337.

(13) Templeton, J. L.; Caldarelli, J. L.; Feng, S.; Philipp, C. L.; Wells, M. B.; Woodworth, B. E.; White, P. S. *J. Organomet. Chem.* **1994**, *478*, 103.

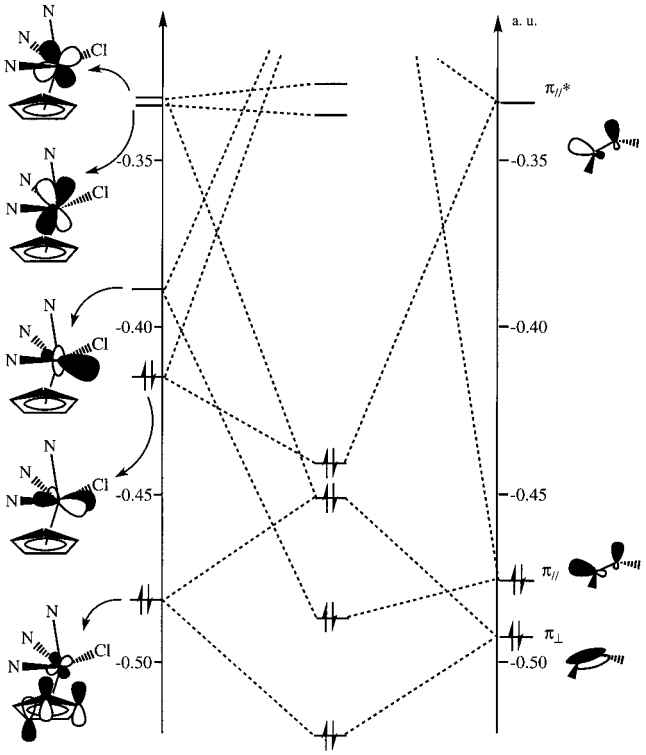

Figure 4. Molecular orbital diagram for the model compound TpCpNbCl(HC≡CH) (1 au = 27.2 eV).

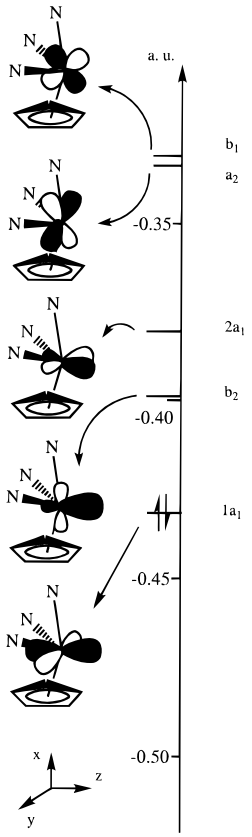

Figure 5. Molecular orbital diagram for the fragment $TpCpNb^+$ (1 au = 27.2 eV).

It constitutes the LUMO of the alkyne complex with virtually no energy change. A very large HOMO−LUMO gap of 2.8 eV is computed. Just above, the second vacant orbital contains some Cp and pyrazole contributions. Interestingly, it points toward the alkyne and has the correct symmetry to interact with the alkyne $\pi_{\perp}$. However, the energy difference between these two orbitals is 4.5 eV, a gap which precludes any notable interaction.

It is worth considering here the status of the alkyne $\pi_{\perp}$ in the complex. This orbital combines with a symmetry-related orbital of the fragment which is Cp−metal bonding. Since these two orbitals are occupied, the high-energy combination receives two electrons from the Cp and the alkyne $\pi_{\perp}$, and its energy is close to that of the HOMO in the complex. This molecular orbital is Cp−$\pi_{\perp}$ antibonding. The alkyne indeed behaves as a 2e donor.

Thus, we clearly understand the bonding scheme which leads to the stable conformation in **3a**. If we now rotate the alkyne, we progressively lose the stabilizing π back-bonding. At 90°, the available metal orbital is a vacant high-energy one. Another destabilizing interaction is obvious when the filled alkyne $\pi_{\perp}$ meets the filled HOMO of the TpCpNbCl fragment. This analysis strongly disfavors this conformation on orbital grounds. Steric hindrance certainly cannot be neglected in the upright position, so that the observed geometry is also preferred on steric grounds. However, the phenyl ring in the solid-state structure of **3a** sits between two pyrazole rings, suggesting that the alkyne could adopt the upright conformation in this wedge as well. We have briefly discussed this point in the preceding section.

In one of their seminal papers, Lauher and Hoffmann[11] have analyzed the bonding in the bent-metallocene complexes $Cp_2MX(L)$. The case of the group 5, 18-electron (d^2) complexes was indeed examined through the example of $Cp_2NbEt(C_2H_4)$. Orbital interactions similar to those found for TpCpNbCl(HC≡CH) lead to a stable conformation where both the ethyl group and the ethylene ligands lie in the wedge formed by the Cp_2-Nb moiety, as observed both spectroscopically and crystallographically.[14] The alternative geometry, where the ethylene stands in the upright position, was examined and found to be strongly disfavored on orbital grounds.

We have also carried out calculations on the fragment $TpCpNb^+$ (Figure 5), and its orbitals are fully reminiscent of those of the Cp_2M fragment.[11] Again, the symmetry is lower, although there is a plane of symmetry that contains the pyrazole ring *trans* to the Cp ring (*xz* in Figure 5). We have labeled the orbitals of the $TpCpNb^+$ fragment after the labels of the familiar orbitals of the Cp_2M fragment.[11] Only slight differences in energy and orientation are noticeable for the three low-lying orbitals. The two highest orbitals are almost degenerate and are inverted as compared to Cp_2M. Consequently, an analysis similar to that followed previously[11] for Cp_2M leads first to the diagram of Figure 3, after adding the σ- and π-donor chloride, and then to the diagram of Figure 4, where the σ-donor and π-acceptor alkyne is introduced. It is worth mentioning here that the splitting of orbitals of the $TpCpNb^+$ fragment is entirely comparable to that of the CpCbM fragment (Cb is cyclobutadiene).[15]

(14) Guggenberger, L. J.; Meakin, P.; Tebbe, F. N. *J. Am. Chem. Soc.* **1974**, *96*, 5420.

(15) Curnow, O. J.; Hirpo, W.; Butler, W. M.; Curtis, M. D. *Organometallics* **1993**, *12*, 4479.

Conclusion

In this article we have described the synthesis and structure of several Tp-containing niobium(III) alkyne complexes with 16 valence electrons. Solution and solid-state studies indicate the presence of a mirror plane in these molecules. Extended Hückel calculations suggest that the main reason for this preference does not lie on orbital grounds. Steric requirements have been probed, especially through the study of alkyne rotation barriers but also through reactivity studies. Indeed, the 18-electron niobium(III) complex TpCpNbCl(PhC≡CMe) is formed, but not its Tp* congener. The horizontal geometry adopted by the alkyne in the latter complex stems from both orbital and steric interactions. Finally, mixed TpCp complexes are not common.[16] TpCpV is a unique member among the group 5 metal complexes.[17]

Experimental Section

All reactions and workup procedures were performed under an atmosphere of dried dinitrogen using conventional vacuum line and Schlenk-tube techniques. THF and toluene were dried and distilled by refluxing over sodium−benzophenone under argon. *n*-Hexane and dichloromethane were dried and distilled over CaH_2 under argon. Benzene-d_6, toluene-d_8, and chloroform-*d* were stored over molecular sieves under dinitrogen. ^{1}H NMR data were acquired at 250 or 300 MHz and ^{13}C NMR data at 62.9 or 75.45 MHz. The ^{1}H−^{1}H COSY NMR spectrum of **3a** was obtained at 400 MHz (see Supporting Information). Elemental analyses were performed in the Analytical Service of our laboratories. $NbCl_3$(DME),[18] $NbCl_3$(DME)(alkyne),[5] KTp,[19] and NaCp·DME[20] were synthesized according to published procedures.

Synthesis of TpNbCl$_2$(alkyne) (2a−e). The complexes were synthesized from $NbCl_3$(DME), alkyne, and KTp by following the one-pot procedure previously developed for the Tp* analogs or from the preformed $NbCl_3$(DME)(alkyne) complexes and KTp, a method also available for Tp*.[2] Typical yields are 60−70%.

TbNbCl$_2$(PhC≡CMe) (2a). Anal. Calcd for $C_{18}H_{18}BCl_2N_6Nb$: C, 43.9; H, 3.65; N, 17.0. Found: C, 43.7; H, 3.60; N, 16.9. ^{1}H NMR (250 MHz, toluene-d_8): δ 8.33, 7.29 (both d, J = 2 Hz, 1 H each, Tp 3-C*H* and Tp 5-C*H*), 7.15−6.95 (m, C_6H_5 and Tp C*H*), 5.90 (t, J = 2 Hz, 1 H, Tp 4-C*H*), 5.58 (t, J = 2 Hz, 2 H, Tp 4-C*H*), 3.40 (3 H, ≡CCH_3). ^{13}C NMR (50.32 MHz, chloroform-*d*): δ 253.8 (≡*C*Ph), 231.8 (≡*C*Me), 145.1, 143.7, 135.1, 135.0 (Tp 3-*C*H and Tp 5-*C*H), 136.5 (*ipso*-C_6H_5), 131.3, 130.2, 128.6 (C_6H_5), 106.5, 106.3 (Tp 4-*C*H), 23.9 (≡C*C*H_3).

TpNbCl$_2$(MeC≡CMe) (2b). Anal. Calcd for $C_{13}H_{16}BCl_2N_6Nb$: C, 36.2; H, 3.7; N, 19.5. Found: C, 36.6; H, 3.8; N, 19.0. ^{1}H NMR (300 MHz, benzene-d_6): δ 8.38, 7.27 (both d, J = 2 Hz, 1 H each, Tp 3-C*H* and Tp 5-C*H*), 7.10, 7.06 (both d, J = 2 Hz, 2 H each, Tp 3-C*H* and Tp 5-C*H*), 5.86 (t, J = 2 Hz, 1 H, Tp 4-C*H*), 5.64 (t, J = 2 Hz, 2 H, Tp 4-C*H*), 2.86 (6 H, ≡CCH_3). ^{13}C NMR (75.45 MHz, chloroform-*d*): δ 246.4 (≡*C*Me), 144.4, 143.6, 135.1, 134.9 (Tp 3-*C*H and Tp 5-*C*H), 106.1, 106.0 (Tp 4-*C*H), 22.4 (≡C*C*H_3).

TpNbCl$_2$(EtC≡CEt) (2c). Anal. Calcd for $C_{15}H_{20}BCl_2N_6Nb$: C, 39.3; H, 4.4; N, 18.3. Found: C, 39.1; H, 4.4; N, 18.7. ^{1}H NMR (300 MHz, benzene-d_6): δ 8.36, 7.25 (both d, J = 2 Hz, 1 H each, Tp 3-C*H* and Tp 5-C*H*), 7.18, 7.05 (both d, J = 2 Hz, 2 H each, Tp 3-C*H* and Tp 5-C*H*), 5.84 (t, J = 2 Hz, 1 H, Tp 4-C*H*), 5.63 (t, J = 2 Hz, 2 H, Tp 4-C*H*), 3.26 (t, 4 H, J = 7.5 Hz, ≡CCH_2CH$_3$), 1.18 (q, 6 H, J = 7.5 Hz, ≡CCH$_2$CH_3). ^{13}C NMR (75.45 MHz, chloroform-*d*): δ 247.7 (≡*C*CH$_2$CH$_3$), 145.0, 144.4, 134.7, 134.6 (Tp 3-*C*H and Tp 5-*C*H), 106.4, 106.3 (Tp 4-*C*H), 31.9 (≡C*C*H$_2$CH$_3$), 13.7 (≡CCH$_2$*C*H$_3$).

TpNbCl$_2$(Me$_3$SiC≡CSiMe$_3$) (2d). Anal. Calcd for $C_{17}H_{28}BCl_2N_6NbSi_2$: C, 37.3; H, 5.2; N, 15.4. Found: C, 37.3; H, 5.3; N, 15.5. ^{1}H NMR (300 MHz, toluene-d_8, 190 K): δ 8.29, 7.23 (both d, J = 2 Hz, 1 H each, Tp 3-C*H* and Tp 5-C*H*), 7.31, 6.88 (both d, J = 2 Hz, 2 H each, Tp 3-C*H* and Tp 5-C*H*), 5.66 (t, J = 2 Hz, 1 H, Tp 4-C*H*), 5.49 (t, J = 2 Hz, 2 H, Tp 4-C*H*), 0.91 (s, 9 H, SiCH_3), −0.34 (s, 9 H, SiCH_3). ^{13}C NMR (50.3 MHz, toluene-d_8, 294 K): δ 145.3, 144.1, 134.5, 134.3 (Tp 3-*C*H and Tp 5-*C*H), 106.3, 106.1 (Tp 4-*C*H), −0.24 (Si*C*H$_3$).

TpNbCl$_2$(PhC≡CPh) (2e). Anal. Calcd for $C_{23}H_{20}BCl_2N_6Nb$: C, 49.2; H, 3.6; N, 15.2. Found: C, 49.8; H, 3.6; N, 15.1. ^{1}H NMR (300 MHz, benzene-d_6): δ 8.52, 7.32 (both d, J = 2 Hz, 1 H each, Tp 3-C*H* and Tp 5-C*H*), 7.64−7.21 (m, 10 H, C_6H_5), 7.15, 7.11 (both d, J = 2 Hz, 2 H each, Tp 3-C*H* and Tp 5-C*H*), 5.89 (t, J = 2 Hz, 1 H, Tp 4-C*H*), 5.50 (t, J = 2 Hz, 2 H, Tp 4-C*H*). ^{13}C NMR (75.45 MHz, benzene-d_6): δ 235.0 (≡*C*Ph), 145.8, 144.3, 137.4, 134.6 (Tp 3-*C*H and Tp 5-*C*H), 137.4 (*ipso*-C_6H_5), 134.5−127.5 (C_6H_5), 106.2, 106.1 (Tp 4-*C*H).

TpCpNb(Cl)(PhCCMe) (3a). THF (30 mL) was added to a mixture of **2a** (0.845 g, 1.7 mmol) and NaCp·DME (0.352 g, 1.98 mmol), and the resulting mixture was stirred for 5 h, during which time it turned from red-purple to orange-brown. Toluene (10 mL) was added and the slurry evaporated to dryness. Extraction with toluene (40 mL), addition of hexanes (10 mL), and filtration through a Celite pad gave an orange-brown solution. Precipitation was induced upon slow concentration followed by addition of hexanes. The resulting microcrystals of **3a** were isolated by filtration, washed several times with hexanes, and then dried under vacuum (yellow microcrystals, 0.680 g, 1.3 mmol, 76%). An analytical sample was obtained after recrystallization from a dichloromethane/hexanes mixture. Anal. Calcd for $C_{23}H_{23}BClN_6Nb$: C, 52.9; H, 4.4; N, 16.1. Found: C, 52.5; H, 4.1; N, 16.0. Assignments in the ^{1}H NMR spectrum have been made possible *via* homodecoupling and COSY ^{1}H−^{1}H experiments. ^{1}H NMR (400.14 MHz, benzene-d_6): major isomer, δ 8.33, 7.53, 7.49, 7.44, 7.12, 6.86 (d, J = 2 Hz, 1 H each, Tp 3-C*H* and Tp 5-C*H*), 7.07−6.98 (m, 3H, C_6H_5), 6.06 (m, 2H, C_6H_5), 6.05, 5.77, 5.66 (t, J = 2 Hz, 1 H each, Tp 4-C*H*), 5.42 (s, 5H, C_5H_5), 3.19 (s, 3 H, ≡CCH_3); minor isomer (some resonances obscured), δ 8.36 (d, J = 7 Hz, 2 H, *o*-C_6H_5), 7.58 (t, J = 7 Hz, 2H, *m*-C_6H_5), 7.22 (t, J = 7 Hz, 1 H, *p*-C_6H_5), 8.30, 7.41, 7.40 (d, J = 2 Hz, 1 H, Tp 3-C*H* and Tp 5-C*H*), 6.11, 6.03, 5.53 (t, J = 2 Hz, 1 H each, Tp 4-C*H*), 5.57 (s, 5H, C_5H_5), 2.09 (s, 3 H, ≡CCH_3). Isomer ratio: 5:1. In toluene-d_8 at 373 K the ≡CCH_3 signals were markedly broadened. ^{13}C{^{1}H} NMR (50.32 MHz, benzene-d_6): major isomer, δ 163.5, 152.9 (≡*C*Ph and ≡*C*CH$_3$), 147.6, 146.5, 144.8, 136.2, 134.6, 132.2 (Tp 3-*C*H and Tp 5-*C*H), 142.4 (*ipso*-C_6H_5), 128.0, 126.6, 125.4 (C_6H_5), 109.9 (C_5H_5), 105.6, 105.5, 104.2 (Tp 4-*C*H), 16.6 (≡C*C*H$_3$); minor isomer, δ 162.8, 156.3 (≡*C*Ph and ≡*C*CH$_3$), 146.7, 146.2, 145.3, 136.4, 134.3, 132.1 (Tp 3-*C*H and Tp 5-*C*H), 138.4 (*ipso*-C_6H_5), 131.2, 128.3, 127.1 (C_6H_5), 109.2 (C_5H_5), 105.9, 105.4, 104.4 (Tp 4-*C*H), 16.9 (≡C*C*H$_3$).

X−ray Crystallographic Analyses. The diffraction data for compounds **2a** and **3a** were collected at 293 K on a four-circle ENRAF-Nonius CAD 4 diffractometer using Mo Kα radiation and a graphite monochromator. Unit cell dimensions with standard deviations were obtained from a least-squares refinement of the setting angles of 25 well-centered reflections. Three standard reflections were checked periodically. They showed no change during data collection. Details are summarized in Table 1. Corrections were made for Lorentz and polarization effects. Empirical absorption corrections (DIFABS) were applied.[21] Computations were performed by using CRYSTALS[22] adapted on a PC. The atomic scattering factors

(16) (a) Trofimenko, S. *Chem. Rev.* **1993**, *93*, 943. (b) Trofimenko, S. *Prog. Inorg. Chem.* **1986**, *34*, 115.
(17) Manzer, L. E. *J. Organomet. Chem.* **1975**, *102*, 167.
(18) Roskamp, E. J.; Pedersen, S. F. *J. Am. Chem. Soc.* **1987**, *109*, 6551.
(19) Trofimenko, S. *J. Am. Chem. Soc.* **1967**, *89*, 3170.
(20) Braunstein, P.; Bender, P.; Jud, J.-M. *Inorg. Synth.* **1989**, *26*, 341.
(21) Walker, N.; Stuart, D. *Acta Crystallogr.* **1983**, *A39*, 158.

were taken from the literature.[23] The structure was solved by direct methods (SHELXS 86)[24] and subsequent difference Fourier maps. Hydrogen atoms were located by Fourier syntheses, but their coordinates (except for those of H(1)) were introduced in the process of refinement as fixed contributors in calculated positions (C−H = 0.98 Å), with fixed thermal parameters 20% higher than that of the carbon to which they were attached. Atomic coordinates and thermal parameters for H(1) were isotropically refined. All non-hydrogen atoms were anisotropically refined, excepted for **2a·thf**, where the THF carbon atoms were refined isotropically. Full-matrix least-squares refinement was carried out minimizing the function $\sum w(|F_o| - |F_c|)^2$, where F_o and F_c are the observed and calculated structure factors, respectively. Selected bond distances and angles are provided in Tables 2 and 3, for **2a·thf** and **3a**, respectively.

EHMO Calculations. Standard EHMO calculations were carried out using the CAChe system with conventional H_{ii} values and a double-ζ basis set for Nb. The model compounds $TpNbCl_2(HC{\equiv}CH)$ and $TpCpNbCl(HC{\equiv}CH)$ were considered with the bond lengths and angles taken from the X-ray structures of **2a** and **3a**. The acetylene C−H bond length was set at 1.10 Å.

Acknowledgment. We thank Acciones Integrada Program PICASSO 94−95 (Spain−France) for traveling grants. J.F.B., F.J., A.O., and M.E.R.B. thank the Direccion General de Investigaciones Cientificas (DGICyT) (Grant No. 92-0715) for support. M.E. wishes to thank Dr. Odile Eisenstein (Orsay, France) and Dr. Alain Klotz (Toulouse, France) for helpful discussions about the EHMO results. Insightful comments by the reviewers are also acknowledged. Electrochemical measurements have been carried out by Dr. Dominique de Montauzon (Service d'Electrochimie, LCC CNRS).

Supporting Information Available: Figures giving the low-field part of the ^1H and corresponding $^1H-^1H$ COSY NMR spectra of **3a** and tables and text giving full details of the X-ray structure determinations for **2a** and **3a** (17 pages). Ordering information is given on any current masthead page.

OM960404T

(22) Watkin, D. J.; Carruthers, J. R.; Betteridge, P. W. *Crystals Users Guide*; Chemical Crystallography Laboratory, University of Oxford: Oxford, U.K., 1985.

(23) *International Tables for X-Ray Crystallography*; Kynoch Press: Birmingham, U.K., 1974; Vol. IV.

(24) Sheldrick, G. M. SHELXS-86 Program for Crystal Structure Solution; University of Göttingen, Göttingen, Germany, 1986.